OPTICS

Observation of twist-induced geometric phases and inhibition of optical tunneling via Aharonov-Bohm effects

Midya Parto, Helena Lopez-Aviles, Jose E. Antonio-Lopez, Mercedeh Khajavikhan, Rodrigo Amezcua-Correa, Demetrios N. Christodoulides*

Geometric phases appear ubiquitously in many and diverse areas of the physical sciences, ranging from classical and molecular dynamics to quantum mechanics and solid-state physics. In the realm of optics, similar phenomena are known to emerge in the form of a Pancharatnam-Berry phase whenever the polarization state traces a closed contour on the Poincaré sphere. While this class of geometric phases has been extensively investigated in both free-space and guided wave systems, the observation of similar effects in photon tunneling arrangements has so far remained largely unexplored. Here, we experimentally demonstrate that the tunneling or coupling process in a twisted multicore fiber system can display a chiral geometric phase accumulation, analogous to the Aharonov-Bohm effect. In our experiments, the tunneling geometric phase is manifested through the interference of the corresponding supermodes. Our work provides the first observation of Aharonov-Bohm suppression of tunneling in an optical setting.

INTRODUCTION

Quantum tunneling plays a central role in a number of intriguing phenomena in physics (*1*–*3*). An archetypical manifestation of this quantum effect is the possibility of electron tunneling between multiple quantum wells when separated by potential barriers. On many occasions, even this simple class of systems can exhibit some unexpected quantum behaviors. For instance, complete quenching of coherent quantum tunneling can be achieved by appropriately imposing a time-harmonic drive to a double-well potential or other more complex lattice systems (*4*–*6*). Another intriguing process is that arising from the topological restoration of energy degeneracies associated with bound states. These effects can reveal themselves in multiple quantum wells that are arranged on a closed loop, when threaded by a constant magnetic flux of certain quantized magnitudes (*7*). This occurs because of the interference between degenerate electronic wave functions, when a nonzero Aharonov-Bohm (AB) phase is accumulated (*8*). However, despite early theoretical efforts, an experimental observation of this latter effect is still lacking, as of yet, within the context of solid-state physics, primarily due to practical challenges associated with the need for ultrahigh magnetic fluxes.

In recent years, the realization of synthetic gauge fields in physical settings involving neutral entities has provided a flexible platform to observe dynamics similar to those arising from the interaction of electrons with magnetic fields (*9*, *10*). In general, such artificial magnetism can be achieved either through dynamic temporal/spatial modulation of the couplings (*11*–*14*) or via the use of geometric phases (*15*, *16*). So far, this artificial magnetism has led to the demonstration of photonic topological insulators in both passive (*13*, *17*, *18*) and active arrangements (*19*), Landau levels for photons (*20*, *21*), and quantum many-body effects (*22*). An important advantage offered by such schemes is the possibility for experimental demonstrations of a certain class of quantum phenomena without invoking magnetic fields, something that would have been otherwise impossible within the context of condensed matter physics. In optics, perhaps the earliest demonstration of a geometric phase is that associated with polarized light (*23*). This arises when the polarization state of light follows a closed contour on the Poincaré sphere. As a result, the corresponding electric field amplitude acquires a geometric phase, known as the Pancharatnam-Berry phase (*23*, *24*). Similar effects can also occur for linearly polarized light (*25*) or speckle patterns in a multimode optical fiber (*26*, *27*), when the direction of propagation varies in space.

Here, we experimentally demonstrate an optical geometric phase that is associated with photon tunneling in a twisted multicore fiber structure. We show that this form of geometric phase results from a constant rotation in the local frame of the fiber and appears in a chiral manner in the corresponding coupling coefficients between adjacent cores. Thus far, twisted photonic crystal fibers have been used to demonstrate coreless light guiding, optical activity, and orbital angular momentum conservation (*28*–*30*). Alternatively, in our study, we use the twist-induced geometric phase to realize a synthetic magnetic field for the photon coupling between nearest-neighbor light channels. As proposed in recent studies (*31*–*34*), this is analogous to the AB effect associated with electron dynamics in the presence of a magnetic flux. We further exploit this analogy to demonstrate the AB suppression of light tunneling in a four-core twisted optical fiber. While this latter effect was originally predicted in the context of quantum electronics (*7*), its experimental observation has so far remained elusive due to the requirement of strong magnetic fields. In this regard, it is only recently that an experimental observation of this type has been reported in a system involving ultracold Ca ions in a linear Paul trap (*35*). In our experiments, we investigate the effect of different twist rates, emulating synthetic gauge fields of varying magnitudes. In this respect, the conditions for a complete tunneling inhibition are investigated, both theoretically and experimentally. Our experimental results are in good agreement with those expected from theory for different twist rates. Moreover, we study the behavior of this same arrangement under high-power conditions, where nonlinear effects start to antagonize the coupling mechanisms in the multicore system. In this highly nonlinear regime, we find that the suppression of tunneling still persists, a direct by-product of the topological nature of the AB geometric phase.

CREOL, The College of Optics & Photonics, University of Central Florida, Orlando, FL 32816, USA.
*Corresponding author. Email: demetri@creol.ucf.edu

Lastly, even in the case where each core is multimoded, we demonstrate that the AB inhibition of tunneling occurs in a universal fashion. In other words, this same process can totally eliminate the coupling for all higher-order modes.

RESULTS

A twisted multicore fiber platform for realizing synthetic magnetic fields for photons

To demonstrate AB suppression of light tunneling because of geometric phase effects, we fabricated a four-core optical fiber structure as shown in the inset of Fig. 1. Each of the four circular cores is coupled to its nearest neighbors, while a fluorine-doped refractive index depression in the middle of the structure eliminates any cross-channeling effects between opposite cores (see Materials and Methods). An artificial gauge field is then imposed on this system after twisting the multicore fiber. In this case, the evolution of the optical modal field amplitudes is described by a paraxial wave equation, expressed in the twisted local frame, in a way analogous to that associated with electron wave functions in the presence of a magnetic field (Fig. 1) (*16*, *31*, *36*). In quantum mechanics, in the presence of a uniform magnetic field, a gauge transformation through Peierls substitution is known to reduce the electron dynamics to those expected under conventional zero-field conditions. This result can be directly extended in more complicated settings such as, for example, atomic lattices. By treating this configuration within the tight-binding formalism, one can then show that the magnetic field now manifests itself in the form of complex coupling coefficients, having phase factors given by the Peierls integral (*37*). Similarly, in a twisted multicore fiber configuration, the coupling coefficients appearing in the coupled mode equations are accordingly modified as $\kappa_{mn}e^{i\varphi_{mn}}$, where κ_{mn} represents the coupling or tunneling strength between subsequent cores in the absence of twisting, while the pertinent phase factor in the tight-binding regime is given by

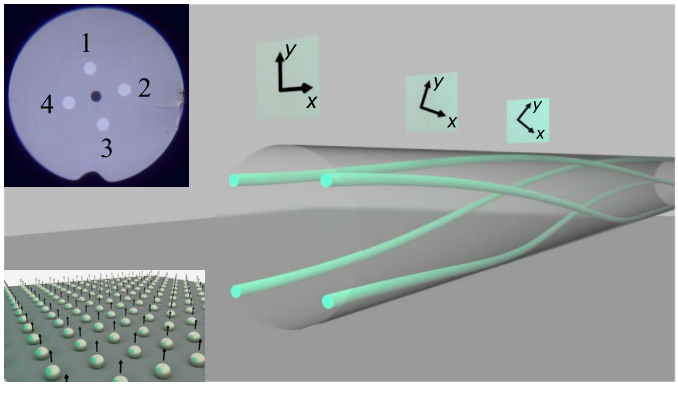

Fig. 1. Twisted fiber structures as a platform for realizing synthetic magnetic fields for photons. A twisted four-core optical fiber in which the photon tunneling evolution dynamics are analogous to those expected from electrons in the presence of a magnetic field. The constantly rotating local transverse coordinates are depicted at three different planes. The top inset shows a microscope image of the input facet of the four-core fiber used in our experiments. The low-index fluorine-doped core is visible at the center of the fiber. The bottom inset depicts a schematic of a two-dimensional atomic lattice in the presence of a static perpendicular magnetic field (arrows), where a tight-binding formalism can be used to describe the electronic band structure after a Peierls substitution.

$$\varphi_{mn} = k_0 \int_{\vec{r}_m}^{\vec{r}_n} \frac{1}{2}\vec{r} \times \vec{B}_{\text{eff}} \cdot \vec{dl} \tag{1}$$

where $\vec{B}_{\text{eff}} = -2n_0\epsilon\hat{z}$ is the effective magnetic field induced by twisting and $\epsilon = 2\pi/\Lambda$ is the angular twist rate. Λ denotes the spatial pitch associated with this helical structure, k_0 represents the free-space wave number, n_0 is the refractive index of the cladding region, and $\vec{r}_{m,n}$ stands for the positions of the neighboring cores m, n. Under these conditions, the evolution of the modal field amplitudes E_n within the cores is given by $id|\psi\rangle/dz + H|\psi\rangle = 0$,where $|\psi\rangle = [E_1, E_2, E_3, E_4]^T$ represents a complex state vector whose evolution is subjected to a Hamiltonian H that is given by

$$H = \begin{pmatrix} \beta_1 & \kappa e^{-i\phi} & 0 & \kappa e^{i\phi} \\ \kappa e^{i\phi} & \beta_2 & \kappa e^{-i\phi} & 0 \\ 0 & \kappa e^{i\phi} & \beta_3 & \kappa e^{-i\phi} \\ \kappa e^{-i\phi} & 0 & \kappa e^{i\phi} & \beta_4 \end{pmatrix} \tag{2}$$

In Eq. 2, β_n stands for the propagation constants of the individual cores, κ is the magnitude of the nearest-neighbor coupling coefficient, while $\phi = (k_0\, n_0\, \epsilon D^2)/2$ represents the AB tunneling phase introduced by the twist, when the core distance between successive sites is D, and $\epsilon = 2\pi/\Lambda$. In the four-core structure prepared, all cores are identical, and so are the respective propagation constants β_n. In this case, the β terms can be readily eliminated from the evolution equations through a trivial gauge transformation. As we will see, however, this is no longer valid under nonlinear conditions.

Controlling and suppressing optical tunneling via twist-induced geometric phases

Equation 2 suggests that photon tunneling in a twisted multicore fiber arrangement is accompanied by a geometric phase accumulation, akin to that expected in electron dynamics from a path-dependent AB phase. To experimentally observe the ϕ phase in the four-core fiber structure, we initially excite core #1 with coherent light from an external cavity laser, operating at $\lambda = 1550$ nm with an output power of ~ 1 mW. The coupling length (L_c) between successive cores is estimated to be ≈ 9 cm. We then monitor the optical power coupled to the opposite core #3, as we vary the magnitude of the effective magnetic field (resulting from different twist rates). At the same time, the power levels in core #2 and core #4 are also recorded. It is important to note that the multicore fiber used here is designed in such a way that, at $\lambda = 1550$ nm, only the fundamental LP_{01} mode is supported by each of the individual cores (Materials and Methods). Figure 2 shows experimental results where the output intensity from core #3 is plotted against the AB phase ϕ. In this same figure, the expected theoretical behavior (see Materials and Methods) as obtained after directly solving the dynamical evolution equations is also presented. These observations indicate that the AB-like suppression of light tunneling from core #1 to core #3 occurs when the gauge field corresponds to $\phi = \pi/4$. This is formally analogous to AB suppression of tunneling for electrons in the presence of a specific magnetic flux. These results provide the first observation of this intriguing effect in an optical setting.

Impact of nonlinearity on AB tunneling inhibition

We further explore how the aforementioned AB-like suppression of tunneling is affected by the Kerr nonlinearity of these silica multicore

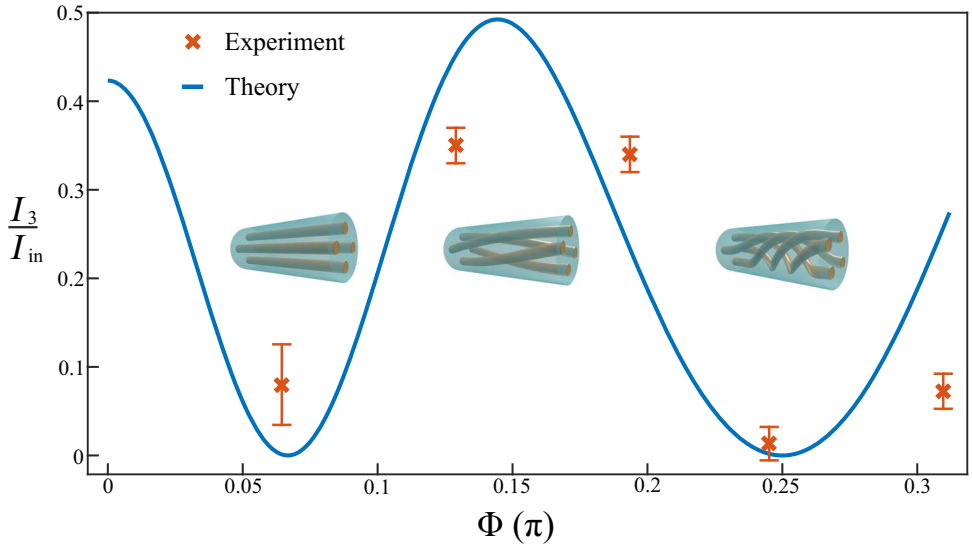

Fig. 2. Dependence of optical tunneling dynamics on the AB phase. Normalized light intensity at the output of core #3 for different values of the AB phase ϕ (as induced by different twist rates). In all cases, core #1 is excited at the input with CW laser light at λ = 1550 nm. Theoretical results corresponding to the same set of parameters are also provided for comparison. At ϕ = π/4, the third core always remains dark, indicating AB tunneling suppression.

fibers. In this respect, we launch ~400-ps high-intensity pulses at λ = 1064 nm from a Q-switched microchip laser into core #1. At this wavelength, the fiber cores in our structure support LP_{11} modes in addition to the fundamental LP_{01}. Because of mode confinement, the LP_{11} modes are very strongly coupled at 1064 nm, while the LP_{01} modes are virtually uncoupled. The initial ratio between the powers launched in LP_{01} and LP_{11} at core #1 is adjusted by cleaving the input facet of the fiber at an angle. In this experiment, the sole purpose of exciting the fundamental LP_{01} mode is to introduce a variable "energy" detuning $\Delta\beta_{NL} = k_0 n_2 |E_{max}|^2$ in the cores, thus allowing us to study how the nonlinearity n_2 affects the inhibition of tunneling dynamics of the LP_{11} modes. This is achieved through cross-phase modulation effects in each core. To observe these effects, we performed intensity measurements both at low ~500-W and high ~6-kW power levels (Materials and Methods). Figure 3 depicts the output intensity profiles at the end of the four-core fiber for different twist-induced phases ϕ. As indicated by these results, at ϕ = π/4, the AB-like inhibition of tunneling between opposite cores still takes place regardless of the optical power exciting this system. In agreement with previous theoretical studies, these observations suggest that this process remains unaffected even under highly nonlinear conditions (*32*). This robustness can be understood through a formal perturbation analysis (Supplementary Materials), indicating that, to first-order, any Δβ variations (linear or nonlinear) within the four cores do not affect the twist-induced degeneracy between the two groups of supermodes at ϕ = π/4. This faithful tunneling inhibition is attributed to the topological nature of this optical AB phase. Lastly, as the optical power injected in the first core increases, a discrete soliton forms around this waveguide channel, further suppressing any tunneling of light to the nearby cores, as also evident in Fig. 3.

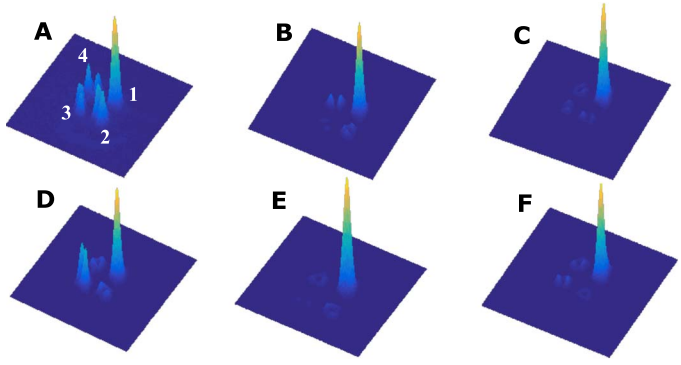

Fig. 3. AB inhibition of tunneling in the presence of optical nonlinearities. Output light intensity profiles from a twisted, 24-cm-long, four-core fiber when only core #1 is quasi-linearly excited for (**A**) ϕ = 0 (no twist), (**B**) ϕ = π/4, and (**C**) ϕ ≈ 0.27π. In (A) to (C), the pulses used had a peak power ~500 W at λ = 1064 nm. (**D**) to (**F**) show similar results when the input peak power is ~6 kW, and hence, nonlinear Kerr effects are at play. It is evident that the coupling between core #1 and core #3 is completely suppressed in both cases (B and E), regardless of the power levels used, indicating an immunity of the AB tunneling suppression against nonlinear index changes. For higher input powers (D to F), the self-focusing nonlinearity further suppresses light coupling, even among adjacent cores. The numbers in (A) depict the relative arrangement of the four cores in this particular experiment.

Tunneling suppression in higher-order spatial modes

It would also be useful to investigate the universality of this class of effects even in multimode environments. To do so, we used a continuous wave (CW) input excitation at λ = 665 nm, where each core can now support four different sets of modes (LP_{01}, LP_{11}, LP_{21}, and LP_{02}). The input power used was ~ 2 mW so as to ensure linear conditions. For this set of parameters, the highest-order propagating mode incited in this system was LP_{02}. Our simulations indicate that, while the coupling coefficients associated with this mode are substantial, all other modes exhibit negligible couplings, at least for length scales involved in our experiment. This is in agreement with experimental observations (Materials and Methods). To study the prospect for AB inhibition of tunneling in this multimode case, we again excite the first core while we record the output intensity patterns corresponding to different values of ϕ. These results are summarized in Fig. 4, where it is evident that the tunneling suppression always occurs, regardless of the number of the modes involved in each individual waveguide element.

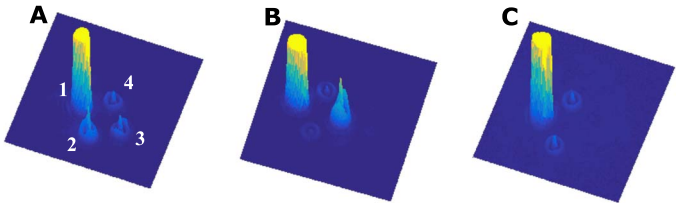

Fig. 4. AB tunneling suppression for higher-order modes. Light intensity distributions at the output of a twisted four-core fiber when the higher-order LP_{02} mode is excited with CW light at $\lambda = 665$ nm. These results are presented for (**A**) $\phi = 0$ (no twist), (**B**) $\phi \approx 0.11\pi$, and (**C**) $\phi = \pi/4$. Although most of the optical power resides in the fundamental LP_{01} mode in the excited core #1, only the LP_{02} mode appears in the remaining cores due to its higher coupling coefficient. (C) reveals that AB suppression of light tunneling occurs in a universal fashion, even for higher-order modes. The numbers in (A) depict the arrangement of the cores corresponding to these observations.

DISCUSSION

According to the AB effect, electron beams acquire a path-dependent phase in their corresponding wave functions in the presence of a nonzero magnetic flux (*8*). This phase shift is not limited to conducting electrons but also arises within the context of quantum tunneling (*7*). Although the AB effect has been observed for electrons in a superconducting or conductive platform (*38*–*40*), its observation in quantum well tunneling settings has so far remained out of reach, mainly due to the demand for high magnetic fluxes, which are experimentally inaccessible. Quite recently, a relevant observation has been reported (*35*), where a linear Paul trap was used to establish a bistable potential with two degenerate eigenstates for Ca ions. A magnetic field was then applied to the structure, and the tunneling rate between the corresponding degenerate states was found to be affected by the associated magnetic flux.

In optics, as originally shown by Pancharatnam, a cyclic change in the polarization of a light beam will, in general, lead to a phase shift accumulated by its corresponding electric field amplitude (*23*). This can be viewed as the equivalent of the AB phase, where the magnetic flux is now replaced by the solid angle subtended by the corresponding cyclic curve on the Poincaré sphere for propagating photons (*24*). On the other hand, the structure implemented here in our study is analogous to the AB effect for tunneling electrons, as predicted in recent theoretical studies (*32*). Here, the uniform twist along a circular multicore fiber acts as a synthetic magnetic field for photon tunneling between adjacent cores. Accordingly, the magnitude of this gauge field can be conveniently varied through mechanical twisting of the fiber, until a complete suppression of coupling between the two opposite cores can be achieved.

As indicated by our experimental results (Fig. 3), the AB tunneling phase in the twisted multicore structure remains invariant regardless of the presence of optical nonlinearity. Moreover, as confirmed by the observations presented in Fig. 4, this same effect happens in a universal manner even for higher-order modes in our optical fiber platform. We would like to emphasize here that local defects in the individual waveguide channels, something inevitable in any experimental realization, would not significantly affect our results (*32*). In other words, this AB-induced tunneling inhibition effect happens to be robust against perturbations. This is attributed to the topological nature of the AB phase, as can be confirmed by perturbation analysis (see the Supplementary Materials). Our observations suggest that similar twisted fiber systems can be envisioned as viable platforms for studying effects akin to those arising from the interaction of electrons with magnetic fields, especially in connection with topological phenomena. Moreover, as suggested in recent studies (*41*, *42*), the role of geometric phases in non-Hermitian settings could lead to novel phenomena in the associated wave dynamics. In this regard, optics provides a viable platform to investigate such aspects. Our results could also contribute to developing new practical schemes for controlling coupling dynamics in multicore optical fibers.

MATERIALS AND METHODS

Four-core optical fiber platform

For our experimental demonstrations, we fabricated a silica fiber consisting of four coupled cores, each with a diameter of ~7.5 μm and a numerical aperture (NA) of 0.12. The neighboring elements were separated from each other by a distance (*D*) of 23 μm. To observe the tunneling suppression between opposite cores, it is essential that any cross couplings are suppressed so that the light propagation dynamics in the system are governed by nearest-neighbor interactions. To achieve this, we judiciously incorporated a fluorine-doped low-index core in the center of the fiber, having a diameter of ~5 μm. In the absence of any twist, when core #1 is initially excited, the light intensity in core #1 and core #3 varies along the propagation distance z according to $I_1(z) = \cos^4 \kappa z$ and $I_3(z) = \sin^4 \kappa z$, as obtained after solving the dynamical modal evolution equations when $\phi = 0$. In other words, light tends to tunnel between these two waveguide channels through core #2 and core #4, in a way similar to tunneling of electrons in a multiwell potential arranged on a circular geometry.

Twisting the structure and the dependency of the coupling on the synthetic gauge field

To introduce an artificial "magnetic field" in our arrangement, we twisted the four-core fiber. The fiber was excited at $\lambda = 1550$ nm, with an external cavity laser with a CW output power of ~1 mW. The output intensity profile from the four cores was then recorded on a complementary metal-oxide semiconductor–based infrared beam profiling camera. Moreover, to discern different cores in the structure, we used a visible imaging camera to capture both the input and output facets of the fiber, once it was twisted. In general, for a given twisting rate (corresponding to an AB phase of ϕ), the light intensity in core #1 and core #3 is explicitly given by the expression

$$I_{1,3}(L) = \frac{1}{4}\left[\cos(2\kappa L \cos\phi) \pm \cos(2\kappa L \sin\phi)\right]^2 \quad (3)$$

where L is the length of the four-core fiber. Figure 2 depicts these theoretical results along with experimentally observed values for different values of ϕ when $L = 24$ cm. As evident from Eq. 3, for the specific case of $\phi = \pi/4$, the third core will always remain dark, irrespective of the length L, in agreement with our experimental results.

High-power characterization and multimode behavior

For the nonlinear experiments, we used a Q-switched microchip laser emitting high-intensity pulses of duration ~400 ps at a rate of 500 Hz, at $\lambda = 1064$ nm. At this wavelength, the highest-order mode supported by the cores happens to be LP_{11}(see the Supplementary Materials). Our analysis shows that this higher-order mode strongly couples nearest-neighbor elements with an L_c of ≈ 2.5 cm, while the fundamental mode remains nearly uncoupled. As indicated in the Supplementary

Materials, at high peak powers (~6 kW), the Kerr nonlinearity associated with silica in the fiber structure results in a detuning in the propagation constant of the excited core. This strong nonlinearly induced detuning starts to compete with the coupling effects, eventually forming discrete solitons in the excited core. This antagonizing effect of the nonlinearity with respect to light coupling is also evident in our experiments (Fig. 3). Lastly, for $\lambda = 665$ nm, each waveguide is multimoded and the mode with the highest coupling happens to be LP_{02}, exhibiting $L_c \approx 10$ cm (see the Supplementary Materials). This is also evident in the experimental results where the intensity profile of the light coupled is that corresponding to a radially symmetric LP_{02} mode.

SUPPLEMENTARY MATERIALS

Supplementary material for this article is available at http://advances.sciencemag.org/cgi/content/full/5/1/eaau8135/DC1

Section S1. Supermodes of twisted multicore optical fibers
Section S2. Perturbation analysis of the tunneling inhibition
Section S3. Coupling of the fundamental mode and higher-order modes
Section S4. Kerr induced detuning in high powers
Section S5. Coupling suppression of higher-order modes
Fig. S1. Twisted N-core fiber.
Fig. S2. Inhomogeneous couplings among cores.
Table S1. Multimode behavior of the designed four-core fiber.

REFERENCES AND NOTES

1. C. Zener, A theory of the electrical breakdown of solid dielectrics. *Proc. R. Soc. Lond. A.* **145**, 523–529 (1934).
2. L. D. Landau, A theory of energy transfer II. *Phys. Z. Sowjetunion.* **2**, 46–51 (1932).
3. C. Zener, Non-adiabatic crossing of energy levels. *Proc R Soc Lond A.* **137**, 696–702 (1932).
4. F. Grossmann, T. Dittrich, P. Jung, P. Hänggi, Coherent destruction of tunneling. *Phys. Rev. Lett.* **67**, 516–519 (1991).
5. D. H. Dunlap, V. M. Kenkre, Dynamic localization of a charged particle moving under the influence of an electric field. *Phys. Rev. B* **34**, 3625–3633 (1986).
6. A. Szameit, I. L. Garanovich, M. Heinrich, A. A. Sukhorukov, F. Dreisow, T. Pertsch, S. Nolte, A. Tünnermann, Y. S. Kivshar, Polychromatic dynamic localization in curved photonic lattices. *Nat. Phys.* **5**, 271–275 (2009).
7. S. Weigert, Topological quenching of the tunnel splitting for a particle in a double-well potential on a planar loop. *Phys. Rev. A* **50**, 4572–4581 (1994).
8. Y. Aharonov, D. Bohm, Significance of electromagnetic potentials in the quantum theory. *Phys. Rev.* **115**, 485–491 (1959).
9. J. Dalibard, F. Gerbier, G. Juzeliūnas, P. Öhberg, Colloquium: Artificial gauge potentials for neutral atoms. *Rev. Mod. Phys.* **83**, 1523–1543 (2011).
10. Y.-J. Lin, R. L. Compton, K. Jiménez-García, J. V. Porto, I. B. Spielman, Synthetic magnetic fields for ultracold neutral atoms. *Nature* **462**, 628–632 (2009).
11. M. Hafezi, E. A. Demler, M. D. Lukin, J. M. Taylor, Robust optical delay lines with topological protection. *Nat. Phys.* **7**, 907–912 (2011).
12. K. Fang, Z. Yu, S. Fan, Realizing effective magnetic field for photons by controlling the phase of dynamic modulation. *Nat. Photonics* **6**, 782–787 (2012).
13. M. C. Rechtsman, J. M. Zeuner, Y. Plotnik, Y. Lumer, D. Podolsky, F. Dreisow, S. Nolte, M. Segev, A. Szameit, Photonic Floquet topological insulators. *Nature* **496**, 196–200 (2013).
14. S. Mukherjee, M. Di Liberto, P. Öhberg, R. R. Thomson, N. Goldman, Experimental observation of Aharonov-Bohm cages in photonic lattices. *Phys. Rev. Lett.* **121**, 075502 (2018).
15. A. L. Fetter, Rotating trapped Bose-Einstein condensates. *Rev. Mod. Phys.* **81**, 647–691 (2009).
16. S.-M. Cui, Nonadiabatic Berry phase in rotating systems. *Phys. Rev. A* **45**, 5255–5257 (1992).
17. M. Hafezi, S. Mittal, J. Fan, A. Migdall, J. M. Taylor, Imaging topological edge states in silicon photonics. *Nat. Photonics* **7**, 1001–1005 (2013).
18. L. Lu, J. D. Joannopoulos, M. Soljačić, Topological photonics. *Nat. Photonics* **8**, 821–829 (2014).
19. M. A. Bandres, S. Wittek, G. Harari, M. Parto, J. Ren, M. Segev, D. N. Christodoulides, M. Khajavikhan, Topological insulator laser: Experiments. *Science* **359**, eaar4005 (2018).
20. M. C. Rechtsman, J. M. Zeuner, A. Tünnermann, S. Nolte, M. Segev, A. Szameit, Strain-induced pseudomagnetic field and photonic Landau levels in dielectric structures. *Nat. Photonics* **7**, 153–158 (2013).
21. N. Schine, A. Ryou, A. Gromov, A. Sommer, J. Simon, Synthetic Landau levels for photons. *Nature* **534**, 671–675 (2016).
22. I. Bloch, J. Dalibard, W. Zwerger, Many-body physics with ultracold gases. *Rev. Mod. Phys.* **80**, 885–964 (2008).
23. S. Pancharatnam, Generalized theory of interference, and its applications. *Proc. Indian Acad. Sci. Sect. A.* **44**, 247–262 (1956).
24. M. V. Berry, The adiabatic phase and pancharatnam's phase for polarized light. *J. Mod. Opt.* **34**, 1401–1407 (1987).
25. A. Tomita, R. Y. Chiao, Observation of Berry's topological phase by use of an optical fiber. *Phys. Rev. Lett.* **57**, 937–940 (1986).
26. B. N. Baranova, B. Y. Zeld'ovich, Rotation of a ray by a magnetic field. *J. Exp. Theor. Phys.* **59**, 681 (1994).
27. I. V. Kataevskaya, N. D. Kundikova, Influence of the helical shape of a fibre waveguide on the propagation of light. *Quantum Electron.* **25**, 927–928 (1995).
28. R. Beravat, G. K. L. Wong, M. H. Frosz, X. M. Xi, P. S. J. Russell, Twist-induced guidance in coreless photonic crystal fiber: A helical channel for light. *Sci. Adv.* **2**, e1601421 (2016).
29. X. M. Xi, T. Weiss, G. K. L. Wong, F. Biancalana, S. M. Barnett, M. J. Padgett, P. S. J. Russell, Optical activity in twisted solid-core photonic crystal fibers. *Phys. Rev. Lett.* **110**, 143903 (2013).
30. X. M. Xi, G. K. L. Wong, M. H. Frosz, F. Babic, G. Ahmed, X. Jiang, T. G. Euser, P. S. J. Russell, Orbital-angular-momentum-preserving helical Bloch modes in twisted photonic crystal fiber. *Optica* **1**, 165–169 (2014).
31. S. Longhi, Bloch dynamics of light waves in helical optical waveguide arrays. *Phys. Rev. B* **76**, 195119 (2007).
32. M. Parto, H. Lopez-Aviles, M. Khajavikhan, R. Amezcua-Correa, D. N. Christodoulides, Topological Aharonov-Bohm suppression of optical tunneling in twisted nonlinear multicore fibers. *Phys. Rev. A* **96**, 043816 (2017).
33. M. Ornigotti, G. D. Valle, D. Gatti, S. Longhi, Topological suppression of optical tunneling in a twisted annular fiber. *Phys. Rev. A* **76**, 023833 (2007).
34. S. Longhi, Light transfer control and diffraction management in circular fibre waveguide arrays. *J. Phys. B At. Mol. Opt. Phys.* **40**, 4477–4492 (2007).
35. A. Noguchi, Y. Shikano, K. Toyoda, S. Urabe, Aharonov–Bohm effect in the tunnelling of a quantum rotor in a linear Paul trap. *Nat. Commun.* **5**, 3868 (2014).
36. C.-H. Tsai, D. Neilson, New quantum interference effect in rotating systems. *Phys. Rev. A* **37**, 619–621 (1988).
37. R. Peierls, Zur Theorie des Diamagnetismus von Leitungselektronen. *Z. Für Phys.* **80**, 763–791 (1933).
38. A. Tonomura, N. Osakabe, T. Matsuda, T. Kawasaki, J. Endo, S. Yano, H. Yamada, Evidence for Aharonov-Bohm effect with magnetic field completely shielded from electron wave. *Phys. Rev. Lett.* **56**, 792–795 (1986).
39. A. Bachtold, C. Strunk, J.-P. Salvetat, J.-M. Bonard, L. Forró, T. Nussbaumer, C. Schönenberger, Aharonov–Bohm oscillations in carbon nanotubes. *Nature* **397**, 673–675 (1999).
40. H. Peng, K. Lai, D. Kong, S. Meister, Y. Chen, X.-L. Qi, S.-C. Zhang, Z.-X. Shen, Y. Cui, Aharonov-Bohm interference in topological insulator nanoribbons. *Nat. Mater.* **9**, 225–229 (2010).
41. S. Longhi, PT phase control in circular multi-core fibers. *Opt. Lett.* **41**, 1897–1900 (2016).
42. D. Leykam, S. Flach, Y. D. Chong, Flat bands in lattices with non-Hermitian coupling. *Phys. Rev. B* **96**, 064305 (2017).

Acknowledgments

Funding: This work was partially supported by the Office of Naval Research (ONR) (MURI N00014-17-1-2588, N0001416-1-2640, and N00014-18-1-2347), NSF (ECCS-1711230, ECCS-1454531, DMR-1420620, and ECCS-1757025), HEL-JTO (W911NF-12-1-0450), Army Research Office (ARO) (W911NF-12-1-0450), the Air Force Office of Scientific Research (AFOSR) (FA955015-10041 and FA9550-14-1-0037), the Army Research Office (ARO) (W911NF-17-1-0481), the U.S.-Israel Binational Science Foundation (BSF) (2016381), DARPA (D18AP00058, HR00111820042, and HR00111820038), and the Qatar National Research Fund (QNRF) (NPRP 9-020-1-006). **Author contributions:** M.P., H.L.-A., M.K., R.A.-C., and D.N.C. conceived the experiments presented here. J.E.A.-L. and R.A.-C. fabricated the fiber structure. M.P. and H.L.-A. built the optical setup and performed the measurements. R.A.-C., M.K., and D.N.C. supervised the project. All authors contributed equally to the writing of this manuscript. **Competing interests:** The authors declare that they have no competing interests. **Data and materials availability:** All data needed to evaluate the conclusions in the paper are present in the paper and/or the Supplementary Materials. Additional data related to this paper may be requested from the authors.

Submitted 17 July 2018
Accepted 27 November 2018
Published 2 January 2019
10.1126/sciadv.aau8135

Citation: M. Parto, H. Lopez-Aviles, J. E. Antonio-Lopez, M. Khajavikhan, R. Amezcua-Correa, D. N. Christodoulides, Observation of twist-induced geometric phases and inhibition of optical tunneling via Aharonov-Bohm effects. *Sci. Adv.* **5**, eaau8135 (2019).

Observation of twist-induced geometric phases and inhibition of optical tunneling via Aharonov-Bohm effects

Midya Parto, Helena Lopez-Aviles, Jose E. Antonio-Lopez, Mercedeh Khajavikhan, Rodrigo Amezcua-Correa and Demetrios N. Christodoulides

Sci Adv **5** (1), eaau8135.
DOI: 10.1126/sciadv.aau8135